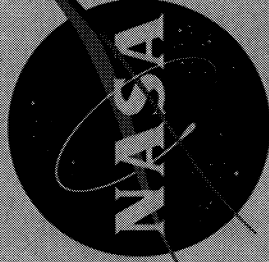


3-28-62  
 REPRODUCED BY AUTHORITY OF NASA  
 DATE 4-21-65  
 CLASSIFICATION CHANGE NO. 14



# CASE FILE

## TECHNICAL MEMORANDUM

X-712

AERODYNAMIC FORCES ON COMPONENTS OF THE X-15 AIRPLANE

By Earl R. Keener and Chris Pembo

Flight Research Center  
 Edwards, Calif.

DECLASSIFIED BY AUTHORITY OF NASA  
 CLASSIFICATION CHANGE NO. 14  
 DATED 4-21-65  
 ITEM NO. 1

CLASSIFICATION CHANGED  
 UNCLASSIFIED

To

Authority of *QC Meyers, II*

Date

*2-5-65*

CLASSIFIED  
 Material containing information of the United States which is exempt from release under the provisions of the Freedom of Information Act, 5 U.S.C. 552, is hereby classified "CONFIDENTIAL" and is to be controlled and handled accordingly.

NATIONAL AERONAUTICS AND SPACE ADMINISTRATION  
 WASHINGTON  
 March 1962

~~CONFIDENTIAL~~

CONFIDENTIAL

## NATIONAL AERONAUTICS AND SPACE ADMINISTRATION

## TECHNICAL MEMORANDUM X-712

## AERODYNAMIC FORCES ON COMPONENTS OF THE X-15 AIRPLANE\* \*\*

By Earl R. Keener and Chris Pembo

## SUMMARY

Aerodynamic force data on the components of the X-15 airplane have been obtained by both pressure and strain-gage measurements in flights covering a Mach number range up to 6.04, altitudes up to about 217,000 feet, and angles of attack up to 15°.

Comparison of the flight data with wind-tunnel data shows generally good agreement for the flight conditions covered.

## INTRODUCTION

In the design of aerospace vehicles which are required to maneuver in the atmosphere, prime factors for consideration are the magnitude and distribution of aerodynamic forces. The design forces and force distributions for the X-15 airplane were obtained from an extensive series of wind-tunnel tests in a relatively unexplored region. An attempt has been made in the flight research program to verify some of the force measurements with both pressure and strain-gage measurements. This paper presents some preliminary results of the flight force data that have been obtained. The data are compared with the wind-tunnel results of reference 1 and with some of the more familiar theoretical methods and approximations.

The flight envelope of the X-15 airplane in terms of Reynolds number plotted against Mach number is shown in figure 1. The solid line shows the maximum performance envelope as determined by a dynamic pressure of 2,500 lb/sq ft at a maximum Mach number and an altitude of 250,000 feet. From this envelope it is anticipated that the flight Reynolds numbers (based on the mean aerodynamic chord of the wing) will

\*This document is based on a paper presented at the Conference on the Progress of the X-15 Project, Edwards Air Force Base, Calif., November 20-21, 1961.

\*\*Title, Unclassified.

DECLASSIFIED BY AUTHORITY OF NASA  
CLASSIFICATION CHANGE NOTICES NO. 124  
DATED 4-21-65 ITEM NO. 1

range from nearly  $50 \times 10^6$  to below 10,000 at altitudes above 250,000 feet. The current flight envelope extends over a Reynolds number range from about  $40 \times 10^6$  down to 60,000. The cross-hatched area shows the flight-test area for aerodynamic-force characteristics. The area is limited by measurement accuracy to altitudes below about 100,000 feet, corresponding to Reynolds numbers greater than about  $5 \times 10^6$ . Wind-tunnel measurements of component forces and surface pressures were obtained at the Reynolds numbers and Mach numbers shown. The bar on the left represents tests at six Mach numbers at nearly constant Reynolds number. The portions of the data published previously are presented in references 1 to 4.

## SYMBOLS

$C_N$	normal force
$C_{N_\alpha}$	normal-force-curve slope, $\frac{\partial C_N}{\partial \alpha}$
$C_{N,WF}$	wing-fuselage normal-force coefficient
$C_{N,WP}$	wing-panel normal-force coefficient
$c$	local wing chord of uncambered section, measured parallel to plane of symmetry
$c_{av}$	average chord of wing panel
$c_n$	wing-section normal-force coefficient, $\int_0^1 \frac{p - p_\infty}{q} \alpha \frac{x}{c}$
$h$	geometric altitude
$M$	free-stream Mach number
$p$	local static pressure
$p_\infty$	free-stream static pressure
$q$	free-stream dynamic pressure
$S_F$	planform area of the fuselage
$S_W$	total area of the wing

$S_{WP}$  area of the exposed wing panel  
 $x$  chordwise distance rearward of leading edge of local chord  
 $\alpha$  angle of attack


### DISCUSSION

Pressure measurements are shown for a wing station near the midsemispan in figure 2. Flight data are shown for an angle of attack of  $10^\circ$  at Mach numbers of 4.7 and 5.4. The wind-tunnel data are shown for comparison at a Mach number of 4.7. In addition, the figure includes unpublished wind-tunnel data for a Mach number of 7.0. A section profile is shown for this wing station. The wing section is a modified NACA 66-005 airfoil, for which the leading-edge radius was increased to 0.375 inch and the trailing-edge thickness was increased to 1-percent chord.

At a Mach number of 4.7, the wind-tunnel data demonstrate that generally good agreement has been obtained between flight and wind-tunnel pressure measurements. At this Mach number the fuselage bow shock crosses the wing near the midsemispan. The effect of the bow shock may be seen on the lower surface by comparing the experimental data with shock-expansion theory for the isolated wing. The experimental data show a pronounced compression as a result of the presence of the bow shock near this station. The data at Mach numbers of 5.4 and 7.0, however, agree with the theory for the isolated wing; thus, it is indicated that the midsemispan is exposed to the free-stream conditions by the inboard movement of the bow shock.

Figure 3 shows the wing-panel spanwise load distribution at a Mach number of 4.7 and angles of attack of  $10^\circ$  and  $15^\circ$ . Both the flight and wind-tunnel data were obtained from pressure measurements at three span stations from which the values of the load parameter  $c_n(c/c_{av})$  were obtained by integration. The flight and wind-tunnel data are in reasonable agreement. Included in this figure is the linear theory for the isolated wing for comparison with the experimental distributions. The theory is shown by the solid line adjusted in level to pass through the data at the midsemispan. The data show that the shape of the distribution of loading can be roughly predicted at these angles of attack by the linear theory for the isolated wing.

The wing-panel normal-force-curve slope as a function of Mach number for low angles of attack is presented in figure 4. Most of the flight data presented were obtained from strain-gage data. Several




points (square data symbols) are also shown which were obtained from flight pressure measurements by integration of span load distributions similar to those of figure 3. The data are compared with linear supersonic theory for the isolated wing. The reduction in slope at supersonic Mach numbers agrees favorably with the linear theory. In addition, the data indicate that the normal force of the wing is about the same as that of an isolated wing for the range of data shown.

It is of interest to mention that the strain-gage data in figure 4 were obtained by using the Bakelite type of gage that has been employed in previous flight research programs. It has been expected that these gages would no longer be useful after the airplane had once exceeded a Mach number of about 4, because of the high temperature. However, the ground calibrations performed after the last flight, which exceeded a Mach number of 6, have shown that the gages were still functioning satisfactorily, even though temperatures above  $500^{\circ}$  F were experienced in the vicinity of some gages. For the data shown, the duration of time covered by the angle-of-attack change was short enough that temperature changes were small.

Figure 5 summarizes the normal-force-curve slopes for trimmed conditions in the angle-of-attack range from  $0^{\circ}$  to  $5^{\circ}$  for the horizontal tail, the wing, the wing-fuselage combination, and the complete airplane. The wing data are the same as those shown in figure 4; however, the coefficients shown in figure 5 are all based on the total wing area of 200 square feet. The slopes shown for the horizontal tail are those obtained from the variation of the balancing-tail load with angle of attack. The balancing-tail loads were obtained from strain-gage measurements during maneuvers, which, in turn, were corrected to zero pitching acceleration to obtain the conditions for balance. Figure 5 can be used to illustrate relative values of component loads for most flight conditions, since the airplane is nearly symmetrical about the horizontal plane. In general, the horizontal-tail load in trimmed flight is about 10 percent of the total airplane load throughout the test range of supersonic speeds. For the portion of the flight program completed, maximum horizontal-tail loads have been well within the design limits.

The normal-force values shown in figure 5 for the wing-fuselage combination were obtained by subtracting the values for the horizontal tail from those for the total airplane. Note that the normal-force slopes for the wing are considerably smaller than those for the wing-fuselage combination. This probably is due, to a large extent, to effects of the fuselage side fairings.

Figure 6 shows the ratio of the wing-panel load to the wing-fuselage load as a function of Mach number, as determined from the data of figure 5. Included in this figure are two approximations based on



H  
2  
4  
4

the planform areas shown. The first approximation of 0.54 is the ratio of the wing-panel area to the total wing area. This approximation is often used at transonic speeds as a rough estimate. The second ratio of 0.27 is the ratio of the wing-panel area to the total wing-fuselage planform area. This approximation may be considered to be roughly applicable at hypersonic speeds. In spite of the rather large scatter in the data, the trend of measured values is to decrease with increasing Mach number from a level near the transonic approximation to a level near the hypersonic approximation.


Figure 7 shows the fuselage pressure distributions over the upper and lower surfaces of the airplane. The conditions shown are for a Mach number of approximately 4.7 and angles of attack of  $0^\circ$  and  $16^\circ$ . The wind-tunnel and flight data are in general agreement at both angles of attack. It is of interest to note the usefulness of the tangent-cone approximation in predicting the positive pressure coefficients. In addition, the two-dimensional Prandtl-Meyer expansion is useful at this Mach number to roughly predict the negative pressure coefficients, approaching a vacuum over the canopy.

Figure 8 shows the pressures on the vertical tail caused by deflecting the speed brakes  $35^\circ$ . The condition shown is for a Mach number of 5.7 at an angle of attack of  $0^\circ$ . Pressures are shown at three stations on the upper vertical tail and at one station on the lower vertical tail. Wind-tunnel results at a Mach number of 4.7 are also presented. The speed-brake hinge line is located at a value of  $x/c$  of 0.65. There is general agreement between wind-tunnel and flight data. The pressures are about the same on both the upper and lower speed brakes. The effect of the speed brakes does not extend appreciably forward or outboard, a fact which is attributed to their low aspect ratio.

Similar data for an angle of attack of  $15^\circ$  are shown in figure 9. Both flight and wind-tunnel data are for a Mach number of 4.7. At this angle of attack the upper speed brake has little effect. This effect is associated with the general blanketing of the upper vertical tail by the wing-fuselage flow field. In contrast, the lower speed brake obtains a higher pressure at an angle of attack of  $15^\circ$  than at an angle of attack of  $0^\circ$ . The large pressure rise still does not result in extensive flow separation ahead of the brake.

#### CONCLUDING REMARKS

Generally good agreement has been obtained between the flight and wind-tunnel measurements for the flight conditions covered. In future



flights the pressure and strain-gage measurements will be extended to higher angles of attack, where interference and nonlinear effects are the predominant flow characteristics.

Flight Research Center

National Aeronautics and Space Administration  
Edwards, Calif., November 20, 1961

#### REFERENCES

1. Hodge, B. Leon, and Burbank, Paige B.: Pressure Distribution of a 0.0667-Scale Model of the X-15 Airplane for an Angle-of-Attack Range of 0° to 28° at Mach Numbers of 2.30, 2.88, and 4.65. NASA TM X-275, 1960.
2. Osborne, Robert S., and Stafford, Virginia C.: Basic Pressure Measurements on a 0.0667-Scale Model of the North American X-15 Research Airplane at Transonic Speeds. NASA TM X-344, 1960.
3. Silvers, H. Norman, Lancaster, Julia A., and Wills, Jane S.: Investigation of the Loading Characteristics of the Lifting Surfaces and the Speed Brakes of a 0.067-Scale Model of the North American X-15 Airplane (Configuration 3) at Mach Numbers of 2.29, 2.98, and 4.65. NASA TM X-301, 1960.
4. Durand, J. A., and Rhudy, J. P.: Heat Transfer and Pressure Distribution Tests on a Model of the X-15 Airplane at Hypersonic Speeds. AEDC-TN-59-63 (Contract No. AF 40(600)-800), Arnold Eng. Dev. Center, July 1959. (Available from ASTIA as AD-307487.)



# FLIGHT ENVELOPE

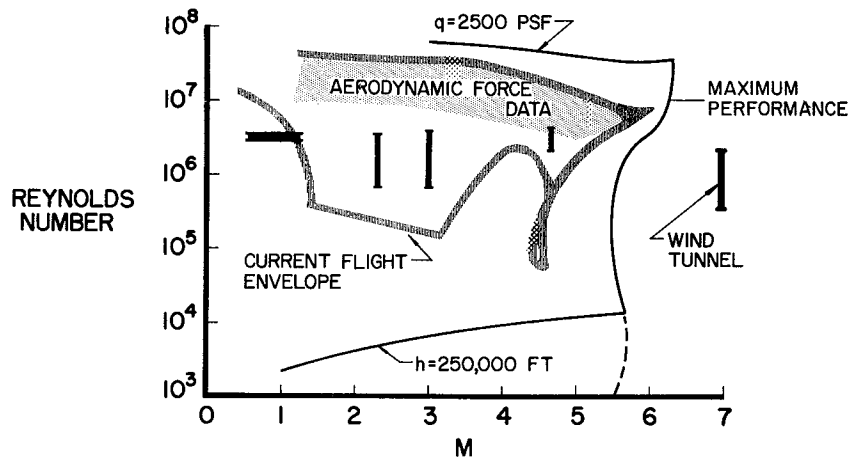


Figure 1

## WING PRESSURE DISTRIBUTION MIDSEMI SPAN $\alpha = 10^\circ$

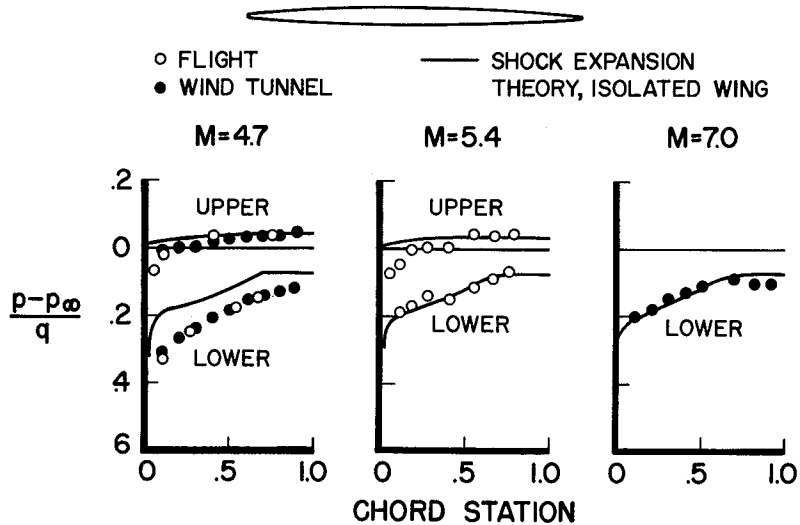


Figure 2



### WING-PANEL SPAN-LOAD DISTRIBUTION $M=4.7$

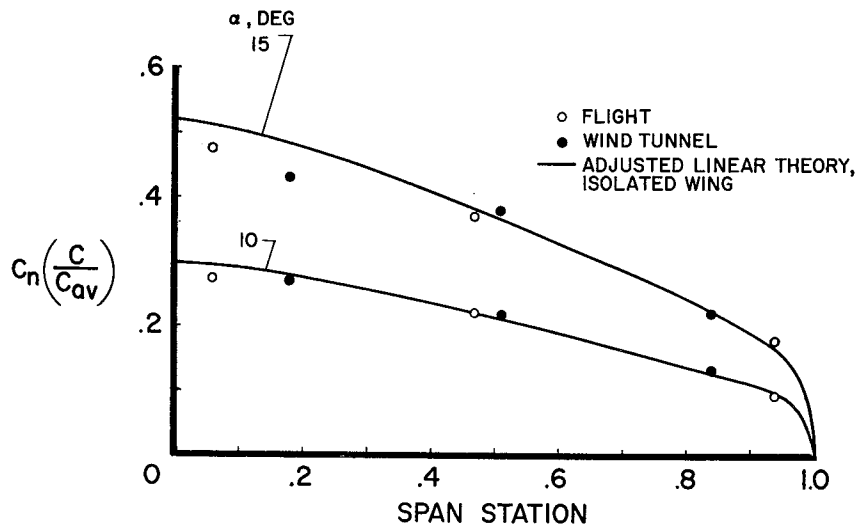


Figure 3

### WING-PANEL NORMAL-FORCE-CURVE SLOPE $\alpha=0^\circ$ TO $5^\circ$

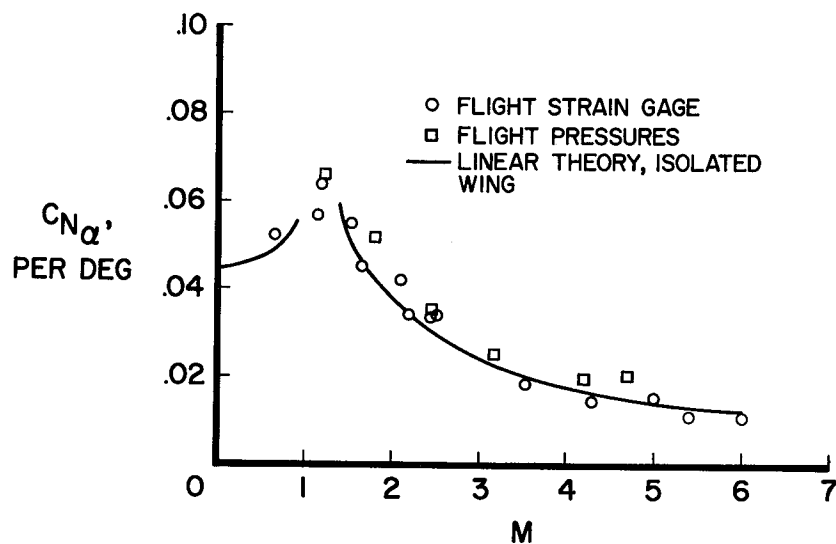


Figure 4

H-244

# DIVISION OF LOADS

$\alpha = 0^\circ \text{ TO } 5^\circ$

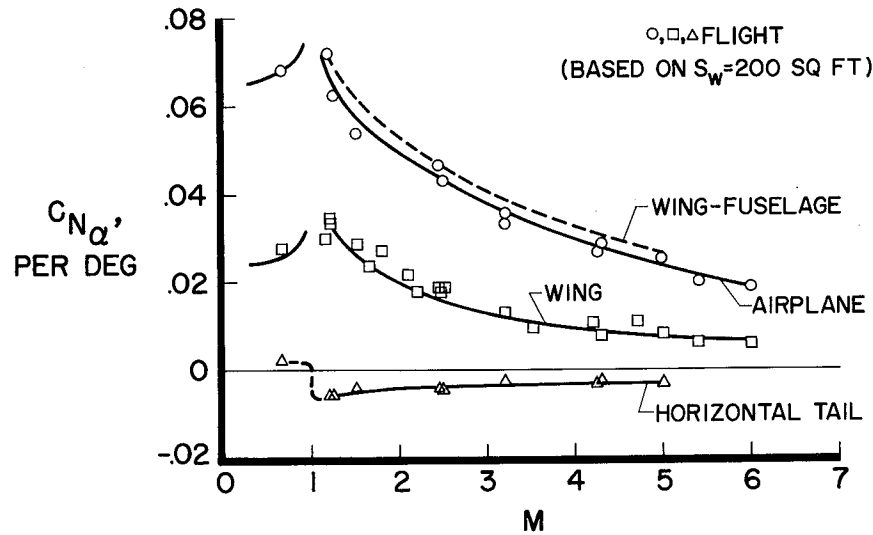


Figure 5

# RATIO OF WING-PANEL LOAD TO WING-FUSELAGE LOAD

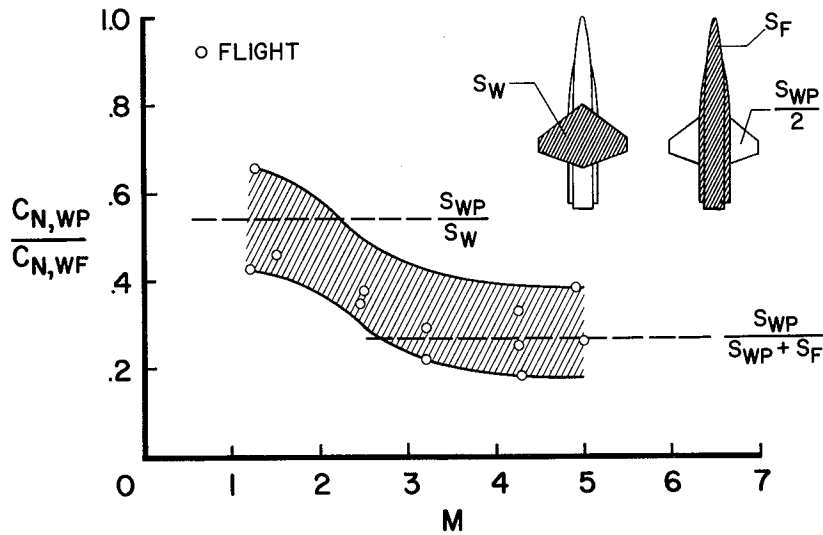


Figure 6

## FUSELAGE PRESSURE DISTRIBUTION

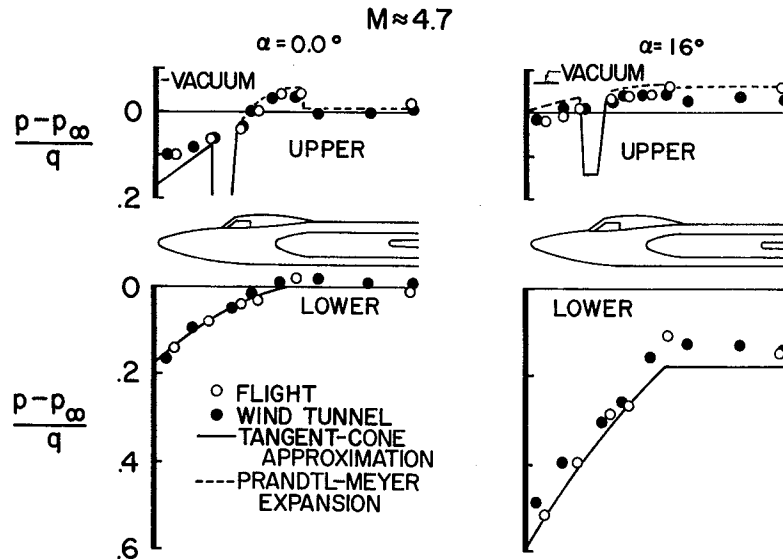


Figure 7

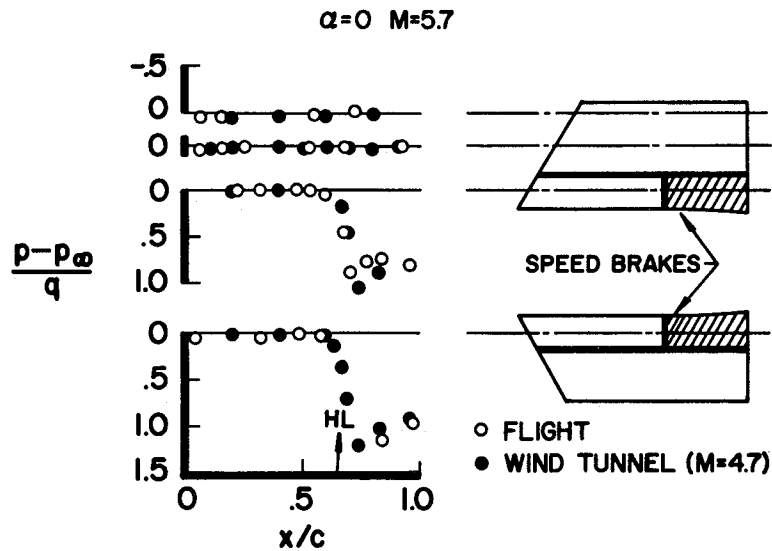
VERTICAL-TAIL PRESSURE DISTRIBUTION  
SPEED BRAKES DEFLECTED  $35^\circ$ 

Figure 8

# VERTICAL-TAIL PRESSURE DISTRIBUTION SPEED BRAKES DEFLECTED 35°

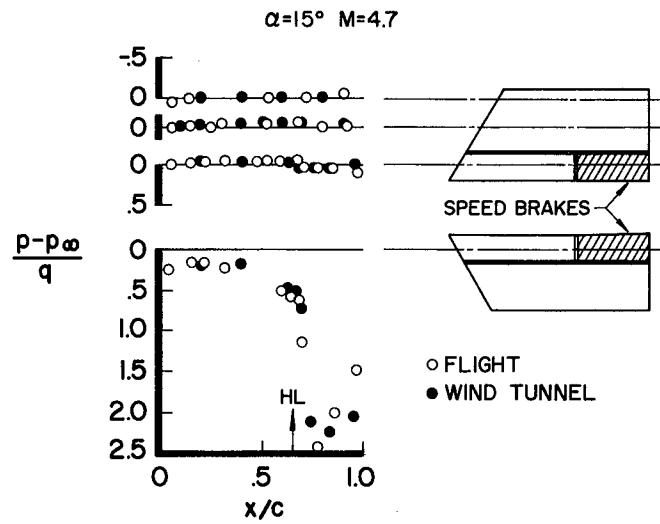


Figure 9

NASA TM X-712

National Aeronautics and Space Administration.  
AERODYNAMIC FORCES ON COMPONENTS OF THE  
X-15 AIRPLANE. Earl R. Keener and Chris Pembo.  
March 1962. 11p.  
(NASA TECHNICAL MEMORANDUM X-712)

(Title, Unclassified)

Aerodynamic force data on the components of the X-15 airplane have been obtained by both pressure and strain-gage measurements in flights covering a Mach number range up to 6.04, altitudes up to about 217,000 feet, and angles of attack up to 15°. Comparison of the flight data with wind-tunnel data shows generally good agreement for the flight conditions covered.

Copies obtainable from NASA, Washington

- ~~CONFIDENTIAL~~
- I. Keener, Earl R.
  - II. Pembo, Chris
  - III. NASA TM X-712

(Initial NASA distribution:  
1, Aerodynamics, aircraft;  
3, Aircraft;  
51, Stresses and loads.)

NASA

NASA TM X-712

National Aeronautics and Space Administration.  
AERODYNAMIC FORCES ON COMPONENTS OF THE  
X-15 AIRPLANE. Earl R. Keener and Chris Pembo.  
March 1962. 11p.  
(NASA TECHNICAL MEMORANDUM X-712)

(Title, Unclassified)

Aerodynamic force data on the components of the X-15 airplane have been obtained by both pressure and strain-gage measurements in flights covering a Mach number range up to 6.04, altitudes up to about 217,000 feet, and angles of attack up to 15°. Comparison of the flight data with wind-tunnel data shows generally good agreement for the flight conditions covered.

Copies obtainable from NASA, Washington

- ~~CONFIDENTIAL~~
- I. Keener, Earl R.
  - II. Pembo, Chris
  - III. NASA TM X-712

(Initial NASA distribution:  
1, Aerodynamics, aircraft;  
3, Aircraft;  
51, Stresses and loads.)

NASA

NASA TM X-712

National Aeronautics and Space Administration.  
AERODYNAMIC FORCES ON COMPONENTS OF THE  
X-15 AIRPLANE. Earl R. Keener and Chris Pembo.  
March 1962. 11p.  
(NASA TECHNICAL MEMORANDUM X-712)

(Title, Unclassified)

Aerodynamic force data on the components of the X-15 airplane have been obtained by both pressure and strain-gage measurements in flights covering a Mach number range up to 6.04, altitudes up to about 217,000 feet, and angles of attack up to 15°. Comparison of the flight data with wind-tunnel data shows generally good agreement for the flight conditions covered.

Copies obtainable from NASA, Washington

- ~~CONFIDENTIAL~~
- I. Keener, Earl R.
  - II. Pembo, Chris
  - III. NASA TM X-712

(Initial NASA distribution:  
1, Aerodynamics, aircraft;  
3, Aircraft;  
51, Stresses and loads.)

NASA

NASA TM X-712

National Aeronautics and Space Administration.  
AERODYNAMIC FORCES ON COMPONENTS OF THE  
X-15 AIRPLANE. Earl R. Keener and Chris Pembo.  
March 1962. 11p.  
(NASA TECHNICAL MEMORANDUM X-712)

(Title, Unclassified)

Aerodynamic force data on the components of the X-15 airplane have been obtained by both pressure and strain-gage measurements in flights covering a Mach number range up to 6.04, altitudes up to about 217,000 feet, and angles of attack up to 15°. Comparison of the flight data with wind-tunnel data shows generally good agreement for the flight conditions covered.

Copies obtainable from NASA, Washington

- ~~CONFIDENTIAL~~
- I. Keener, Earl R.
  - II. Pembo, Chris
  - III. NASA TM X-712

(Initial NASA distribution:  
1, Aerodynamics, aircraft;  
3, Aircraft;  
51, Stresses and loads.)

NASA

NASA TM X-712

National Aeronautics and Space Administration.  
AERODYNAMIC FORCES ON COMPONENTS OF THE  
X-15 AIRPLANE. Earl R. Keener and Chris Pembo.  
March 1962. 11p.

(NASA TECHNICAL MEMORANDUM X-712)

(Title, Unclassified)

Aerodynamic force data on the components of the  
X-15 airplane have been obtained by both pressure  
and strain-gage measurements in flights covering a  
Mach number range up to 6.04, altitudes up to about  
217,000 feet, and angles of attack up to 15°. Com-  
parison of the flight data with wind-tunnel data shows  
generally good agreement for the flight conditions  
covered.

Copies obtainable from NASA, Washington

- ~~CONFIDENTIAL~~
- I. Keener, Earl R.
  - II. Pembo, Chris
  - III. NASA TM X-712

(Initial NASA distribution:  
1, Aerodynamics, aircraft;  
3, Aircraft;  
51, Stresses and loads.)

NASA

NASA TM X-712

National Aeronautics and Space Administration.  
AERODYNAMIC FORCES ON COMPONENTS OF THE  
X-15 AIRPLANE. Earl R. Keener and Chris Pembo.  
March 1962. 11p.

(NASA TECHNICAL MEMORANDUM X-712)

(Title, Unclassified)

Aerodynamic force data on the components of the  
X-15 airplane have been obtained by both pressure  
and strain-gage measurements in flights covering a  
Mach number range up to 6.04, altitudes up to about  
217,000 feet, and angles of attack up to 15°. Com-  
parison of the flight data with wind-tunnel data shows  
generally good agreement for the flight conditions  
covered.

Copies obtainable from NASA, Washington

- ~~CONFIDENTIAL~~
- I. Keener, Earl R.
  - II. Pembo, Chris
  - III. NASA TM X-712

(Initial NASA distribution:  
1, Aerodynamics, aircraft;  
3, Aircraft;  
51, Stresses and loads.)

NASA

NASA TM X-712

National Aeronautics and Space Administration.  
AERODYNAMIC FORCES ON COMPONENTS OF THE  
X-15 AIRPLANE. Earl R. Keener and Chris Pembo.  
March 1962. 11p.

(NASA TECHNICAL MEMORANDUM X-712)

(Title, Unclassified)

Aerodynamic force data on the components of the  
X-15 airplane have been obtained by both pressure  
and strain-gage measurements in flights covering a  
Mach number range up to 6.04, altitudes up to about  
217,000 feet, and angles of attack up to 15°. Com-  
parison of the flight data with wind-tunnel data shows  
generally good agreement for the flight conditions  
covered.

Copies obtainable from NASA, Washington

- ~~CONFIDENTIAL~~
- I. Keener, Earl R.
  - II. Pembo, Chris
  - III. NASA TM X-712

(Initial NASA distribution:  
1, Aerodynamics, aircraft;  
3, Aircraft;  
51, Stresses and loads.)

NASA

NASA TM X-712

National Aeronautics and Space Administration.  
AERODYNAMIC FORCES ON COMPONENTS OF THE  
X-15 AIRPLANE. Earl R. Keener and Chris Pembo.  
March 1962. 11p.

(NASA TECHNICAL MEMORANDUM X-712)

(Title, Unclassified)

Aerodynamic force data on the components of the  
X-15 airplane have been obtained by both pressure  
and strain-gage measurements in flights covering a  
Mach number range up to 6.04, altitudes up to about  
217,000 feet, and angles of attack up to 15°. Com-  
parison of the flight data with wind-tunnel data shows  
generally good agreement for the flight conditions  
covered.

Copies obtainable from NASA, Washington

- ~~CONFIDENTIAL~~
- I. Keener, Earl R.
  - II. Pembo, Chris
  - III. NASA TM X-712

(Initial NASA distribution:  
1, Aerodynamics, aircraft;  
3, Aircraft;  
51, Stresses and loads.)

NASA